

# Quantum Melting of Incommensurate Domain Walls in Two Dimensions

Tsutomu Momoi

*Institute of Physics, University of Tsukuba, Tsukuba, Ibaraki 305-8571, Japan*

(Dated: February 28, 2002)

Quantum fluctuations of periodic domain-wall arrays in two-dimensional incommensurate states at zero temperature are investigated using the elastic theory in the vicinity of the commensurate-incommensurate transition point. Both stripe and honeycomb structures of domain walls with short-range interactions are considered. It is revealed that the stripes melt and become a stripe liquid in a large-wall-spacing (low-density) region due to dislocations created by quantum fluctuations. This quantum melting transition is of second order and characterized by the three-dimensional XY universality class. Zero-point energies of the stripe and honeycomb structures are calculated. As a consequence of these results, phase diagrams of the domain-wall solid and liquid phases in adsorbed atoms on graphite are discussed for various domain-wall masses. Quantum melting of stripes in the presence of long-range interactions that fall off as power laws is also studied. These results are applied to incommensurate domain walls in two-dimensional adsorbed atoms on substrates and in doped antiferromagnets, e.g. cuprates and nickelates.

PACS numbers: 64.70.Rh, 61.44.Fw, 64.70.Dv, 74.20.-z

## I. INTRODUCTION

It has been established that a macroscopic number of domain walls (“discommensurations” or “soliton excitations”) appear in incommensurate states and form a global soliton-lattice structure.<sup>1,2,3,4,5,6,7,8</sup> Two-dimensional (2D) solids of adsorbed atoms on graphite have been studied as a typical example of commensurate-incommensurate phase transitions (C-IC transitions).<sup>9,10,11,12</sup> As 2D incommensurate soliton lattices, theoretical works<sup>2,3</sup> proposed stripe and honeycomb structures, and both of them were observed in experiments.<sup>9,11,13</sup> Since domain walls are made from excess atoms (for heavy walls), the domain-wall mass can be controlled in experiments by changing atoms from Xe to <sup>3</sup>He (or H<sub>2</sub>) and, thereby, quantum fluctuation can be increased. Recently, striped anti-phase domain walls were observed in doped nickel oxides and copper oxides,<sup>14,15</sup> in which the stripe structure shows incommensurate short-range order. The effect of quantum fluctuations on the 2D domain-wall structures was hence attracting attention, but in theoretical understanding, little is known about quantum disordered striped or honeycomb states. Striped domain walls were also found in a frustrated 2D quantum spin system that shows magnetization plateaux.<sup>16</sup>

Neutron scattering measurements in the striped incommensurate phases showed that incommensurability is proportional to the excess density  $\delta n$  in adsorbed atoms<sup>11</sup> and to Sr concentration  $x$  in  $\text{La}_{2-x}\text{Sr}_x\text{CuO}_4$  for the underdoped region,  $x < 1/8$ .<sup>15,17</sup> The nature of one domain wall is, hence, unchanged for the whole density region, and the domain-wall spacing only changes depending on the excess (or hole) density. It was argued for doped antiferromagnets that one domain wall behaves like a quantum elastic string.<sup>18,19,20</sup> In adsorbed atom systems, domain walls are not pinned by the substrate periodic potential, but floating, and hence we can also adopt this

string model to describe the single domain wall.

The stability of domain-wall arrays is controlled by effective interactions between walls and fluctuations among them<sup>4,5</sup>. When the wall-wall repulsive interactions are strong enough, the domain walls form a regular array and thereby becomes a solid with incommensurate long-range order (LRO). In experiments, this LRO is observed as sharp incommensurate Bragg peaks, and in the elastic theory for domain walls<sup>4,5</sup> this LRO is characterized by finite stiffness. On the other hand, when fluctuations are strong, dislocations proliferate and thereby make the domain-wall ordering short ranged. In this case, the domain walls are irregular and show a “liquid”-like behavior with exponential decay of correlations, in which incommensurate scattering peaks have finite width. In the elastic theory, this short-range domain-wall order is characterized by vanishing of stiffness. It was shown that thermal fluctuations induce a phase transition from the striped or honeycomb (ordered) solid to a short-range-ordered liquid at finite temperature and the stripe liquid phase remains until zero temperature at the onset of the C-IC transition.<sup>4,5,7</sup> Quantum fluctuation was not taken into account previously with regard to melting of domain-wall structures.

In the classical theory for domain walls in incommensurate adsorbed atoms, the wall-wall repulsive interaction and the wall intersection energy determine the ground-state phase diagram of domain-wall structures.<sup>3</sup> In the stripe structure, walls with spacing  $l$  repel each other by the exponential interaction<sup>4</sup>  $\alpha \kappa \exp(-\kappa l)$ . Here  $\kappa$  denotes the inverse of the domain-wall width and  $\alpha = c_1 Q a^2 Y$ , where  $c_1$  denotes a constant of order unity,  $Q$  the degeneracy of commensurate domains,  $a$  the unit length of atoms in commensurate domains, and  $Y$  the microscopic Young’s modulus of the adsorbate. At zero temperature, the striped domain walls form a regular

parallel array with the energy per unit area

$$E_s = \frac{\zeta_0 - \zeta}{l} + \frac{\alpha\kappa}{l} \exp(-\kappa l), \quad (1)$$

where  $\zeta_0$  and  $\zeta$  denote the energy and the chemical potential of one wall per unit length. On the other hand, the honeycomb structure has the wall-intersection energy<sup>3</sup>  $f_I$  per intersection. The total energy of a regular honeycomb domain walls per unit area is

$$E_h = \frac{2(\zeta_0 - \zeta)}{\sqrt{3}l} + \frac{4f_I}{3\sqrt{3}l^2} + \frac{\sqrt{3}\alpha\kappa}{l} \exp(-\sqrt{3}\kappa l), \quad (2)$$

where  $l$  is the length of one side of the unit hexagon. For each structure, the length  $l$  is determined by minimizing the energy with fixed  $\zeta$ . The ground-state structure is selected by comparing the energies with determined  $l$ 's. When the intersection energy  $f_I$  is positive, the stripe array is more stable than the honeycomb structure for large wall-spacing  $l$  due to absence of the intersection energy, whereas the honeycomb structure is favored for moderate  $l$  due to rapid decay of the wall-wall interaction. If the intersection energy is negative, only honeycomb states appear in the whole density region.<sup>3</sup>

In this paper, we study quantum fluctuations in domain-wall structures taking account of spontaneous creation of dislocations at zero temperature. We use an elastic theory to discuss striped domain walls or honeycomb ones. Considering the effect of dislocations in the 2+1D space, we discuss a quantum-melting transition of the stripe structure, which occurs as a consequence of the proliferation of dislocations. It is shown that, for a large-wall-spacing region, the striped structure with short-range wall-wall interactions is unstable against quantum fluctuations and becomes a stripe liquid even at zero temperature. This melting transition is a continuous one in the universality class of the three-dimensional (3D) XY model. We point out that this quantum disordered stripe phase was presumably observed in neutron scattering experiments of adsorbed  $H_2$  or  $D_2$  monolayer on graphite,<sup>21</sup> and in those of doped copper oxides and nickel oxides.<sup>15,17</sup> For 2D adsorbed atoms, our results indicate that when the wall intersection energy  $f_I$  is positive, the stripe-liquid phase appears between the commensurate and stripe-ordered phases. The zero-point energies are also estimated for both stripe and honeycomb structures, and finally, possible phase diagrams for incommensurate 2D atoms on surfaces are given for various strength of quantum fluctuations. For convenience of readers, we show the phase diagrams obtained in this paper in Fig. 1 in advance. The inverse of the domain-wall mass  $1/m$  and the excess density  $\delta n$  are taken as variables. The parameter  $1/m$  represents the strength of quantum fluctuations and the limit  $1/m \rightarrow 0$  corresponds to the classical limit. A phase separation occurs in a certain density region between the stripe phases and the honeycomb one. On the other hand, if stripes have long-range wall-wall interactions that fall off

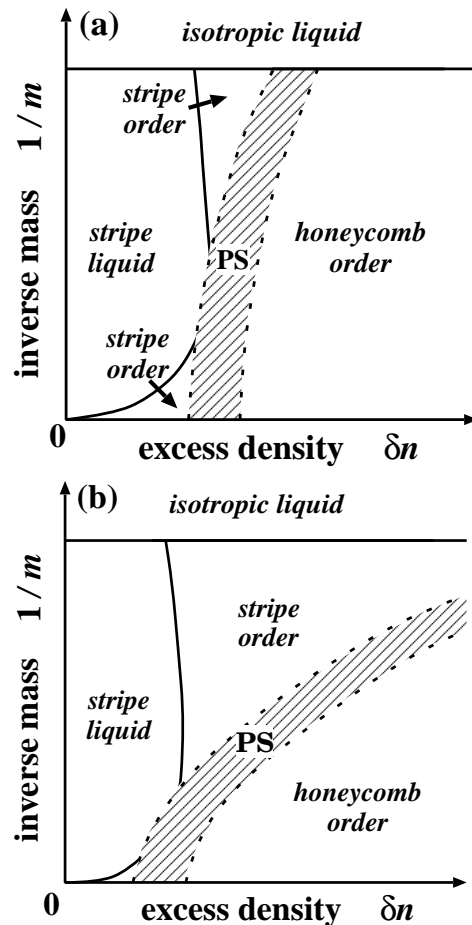


FIG. 1: Schematic phase diagrams of incommensurate phases in 2D adsorbed atoms on substrates. The wall-intersection energy is set to be positive but not very large and the domain-wall width  $\kappa^{-1}$  (a) fixed and (b)  $m$ -dependent. (See text in Sec. IV.) The phase transition between the stripe liquid phase and the stripe ordered one is of second order. In the shaded regions, the phase separation (PS) occurs between the stripe phases and the honeycomb one.

as power laws  $r^{-q+1}$  with  $q < 5$ , the stripe structure is stable in low density and unstable in high density. This tendency to ordering is, thus, opposite to the case of short-range interaction systems.

We discuss the stripe structure with short-range interactions in section II and the honeycomb structure in section III. Phase diagrams for adsorbed atoms on substrates are proposed in section IV. In section V, we discuss stripes with long-range interactions that fall off as power laws. Section VI contains discussions.

## II. STRIPED DOMAIN WALLS

In this section, we discuss quantum fluctuation of stripes and show how a quantum stripe liquid appears.

### A. Hamiltonian of quantum stripes with dislocations

Let us consider first the long-wavelength fluctuations of stripes which do not contain any dislocation. For simplicity, we consider striped domain walls on a rectangular substrate, which are aligned along the  $y$ -axis. It was argued for doped antiferromagnets<sup>18,19,20</sup> that a single domain wall behaves as a quantum elastic string with the wall mass  $m$  per unit length and the interfacial stiffness  $\gamma$ . In adsorbed atom systems, domain walls are floating and hence this string model can be also adopted. Here the mass  $m$  relates to the mass of adsorbed atoms, and the stiffness  $\gamma$  comes from both the line tension of the walls and the anisotropy of substrates. In a stripe pattern, domain walls interact with each other by both the exponential repulsion and hard-core potential, and hence stiffness  $K_x$  appears between walls. In the continuum limit of the displacement field, the Hamiltonian for stripes without any dislocation has the form<sup>22</sup>

$$H_0 = \frac{1}{2} \int d^2r \left\{ \frac{lp^2}{m} + \frac{\gamma}{l} (\partial_y u)^2 + K_x (\partial_x u)^2 \right\} \quad (3)$$

up to quadratic terms, where  $u$  denotes the  $x$  displacement of the wall from the straight position and  $p$  is the conjugate momentum. A path integral representation leads to  $Z_0 = \int \mathcal{D}u(\tau, \mathbf{r}) \exp(-S_0)$  with the effective action

$$S_0[u] = \frac{1}{2\hbar} \int d\tau d^2r \sum_{\alpha=\tau,x,y} K_\alpha (\partial_\alpha u)^2, \quad (4)$$

where  $K_\tau = m/l$  and  $K_y = \gamma/l$ . The functional integral has ultra-violet (UV) momentum cutoffs  $|q_\tau| \leq \pi c/a$ ,  $|q_x| \leq \pi/ql$ , and  $|q_y| \leq \pi/a$ , where  $c \equiv \sqrt{\gamma/m}$ , and  $Q$  denotes the degeneracy of commensurate ground states. With rescaling  $T = c\tau$ ,  $X = (\gamma/lK_x)^{1/2}x$ , and  $Y = y$ , we have the isotropic effective action

$$S_0[u] = \frac{K}{2\hbar} \int dT d^2R \sum_{\alpha=\tau,x,y} (\partial_\alpha u)^2 \quad (5)$$

with  $K = (mK_x/l)^{1/2}$ .

Equation (3) is not the full Hamiltonian, since real stripes have dislocations (defects) even at zero temperature owing to quantum fluctuations. Hence we next take into account the singular part in  $u$  that comes from dislocations. The dislocations become lines (or loops) in the 2+1D space as shown in Fig. 2.  $Q$  domain walls merge together into a dislocation so that each dislocation is consistent with the domain structure. The strength of dislocation lines can be observed<sup>23,24</sup> by a loop integral over derivative of the displacement field on a closed loop  $\Gamma$

$$\oint_\Gamma du = Qls, \quad (6)$$

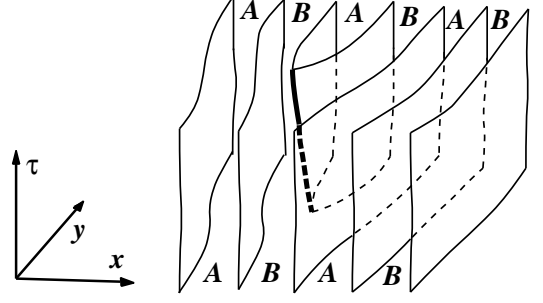


FIG. 2: Dislocation line of stripes in the 2+1D space when the commensurate domains are doubly degenerate ( $Q = 2$ ). Two types of commensurate domains are labelled with A and B.

where  $s$  ( $= 0, \pm 1, \pm 2, \dots$ ) denotes the number of dislocation lines enclosed by the loop  $\Gamma$ . The field  $u$  can be divided into the smooth part  $u_{\text{smooth}}$  and the singular part  $u_{\text{sing}}$  that describes dislocation lines. Thus Fourier transform of the gradient of  $u$  can be written as

$$i\mathbf{q}u_{\text{smooth}}(\mathbf{q}) + iQl\mathbf{q} \times \mathbf{n}(\mathbf{q})/q^2 \quad (7)$$

in the continuum limit, where  $\mathbf{q} = (q_x, q_y, q_\tau)$  and  $\mathbf{n}(\mathbf{q})$  denotes Fourier transform of dislocation density vectors. Inserting eq. (7) into the gradient vector  $\nabla u$  in eq. (5), we obtain the total effective action<sup>23</sup>

$$S = S_0[u_{\text{smooth}}] + S_D[\mathbf{n}] \quad (8)$$

with

$$S_D[\mathbf{n}] = \frac{1}{2\hbar} \int \frac{d^3q}{(2\pi)^3} \frac{(Ql)^2 K}{q^2} |\mathbf{n}(\mathbf{q})|^2. \quad (9)$$

### B. Criterion for quantum melting

After transforming the displacement field as  $\tilde{u} = 2\pi u/Ql$ , the system has periodicity  $2\pi$ . By rescaling  $\tilde{\tau} = c\tau$ ,  $\tilde{x} = ax/ql$  and  $\tilde{y} = y$ , the effective action is

$$S_0 = \frac{1}{2\hbar} \int d\tilde{\tau} d^2\tilde{r} \sum_{\alpha} \tilde{K}_\alpha (\partial_\alpha \tilde{u})^2 \quad (10)$$

with the couplings

$$\begin{aligned} \tilde{K}_\tau &= \tilde{K}_y = Q(Ql)^2 \sqrt{m\gamma}/(2\pi)^2 a, \\ \tilde{K}_x &= (Ql)K_x/(2\pi)^2 ca, \end{aligned} \quad (11)$$

where cutoffs are set as  $\Delta\tilde{\tau} = \Delta\tilde{x} = \Delta\tilde{y} = a$ . In these notations, dislocations are quantized as

$$\oint_\Gamma d\tilde{u} = 2\pi s. \quad (12)$$

The final forms (10) and (12) are equivalent to a spatially anisotropic 3D XY model in the vortex loop

representation.<sup>23,25</sup> Regarding the displacement field as the phase  $\theta(r) = 2\pi u(r)/Ql$ , we thus mapped dislocations of stripes onto vortices of phases, and the 2D quantum stripe system onto the anisotropic 3D XY model with couplings  $2a\tilde{K}_\tau$ ,  $2a\tilde{K}_x$  and  $2a\tilde{K}_y$ .

In the absence of dislocation lines, the Hamiltonian (4) has only quadratic terms, and consequently, the stripes have finite stiffness at any value of parameters  $l$  and  $m$ . Zaanen<sup>22</sup> argued that dislocations cannot proliferate in quantum stripes at zero temperature, but we disagree with his points. His argument about dislocations is based on a classical picture of Kosterlitz-Thouless transition<sup>26</sup> and can be applied only to classical striped systems. Since the quantum system is mapped onto a 2+1D one at finite temperature, gain of quantum entropy can overcome loss of the core energy of dislocations in a specific parameter region. In 3D superfluid, which is equivalent to the 3D XY model, Feynman<sup>27</sup> proposed that vortex loops are responsible for transition. Then it was discussed that dislocation loops reduce superfluidity to zero at the critical temperature.<sup>23,25</sup> This picture was confirmed by Monte Carlo simulations of the 3D XY model<sup>28</sup> and the critical exponent  $\nu = 0.67$  was correctly derived from a renormalization-group treatment of vortex loops.<sup>29</sup>

For the mapped 3D XY model, we know that there are ordered and disordered phases in the parameter space of  $\tilde{K}_\tau$ ,  $\tilde{K}_y$ , and  $\tilde{K}_x$ . It is natural to expect that the critical point is given by the relation

$$(\tilde{K}_x\tilde{K}_y\tilde{K}_\tau)^{1/3}\hbar^{-1} = C \quad (13)$$

with a constant  $C$  of order unity, and long-range order exists for  $(\tilde{K}_x\tilde{K}_y\tilde{K}_\tau)^{1/3}\hbar^{-1} > C$ . Due to the presence of dislocation lines, the stiffness of stripes is reduced and the quantum disordered phase appears in  $(\tilde{K}_x\tilde{K}_y\tilde{K}_\tau)^{1/3}\hbar^{-1} < C$ . This melting is a continuous transition in the same universality class as the 3D XY model. In the stripe-liquid phase, the correlation length shows the form<sup>30</sup>

$$\xi \sim (n_c - n)^{-\nu} \quad (14)$$

with  $\nu \approx 0.67$  near the critical density  $n_c$ . Though there are  $Q$  degenerate ground states for each stripe configuration, they can be changed from one to others by repetition of transformation  $u \rightarrow u + a$  and hence may not affect properties of the phase transition.

### C. Phase diagram

To proceed with calculation of the phase diagram, we need parameter dependence of  $K_x$ . Here, we derive the form of  $K_x$  with various approximations and thereby obtain the phase diagram of the stripe liquid and ordered phases.

In the large- $m$  limit, the wall fluctuation is negligible and the exponential repulsion dominates the stiffness

$$K_x = \alpha\kappa^3 l \exp(-\kappa l). \quad (15)$$

When the mass  $m$  is finite, but large enough, the wall fluctuation slightly modifies the effective repulsion form. Since the quantum elastic string is equivalent to a 3D classical Gaussian surface in the path-integral picture, we can use results derived for the 3D Gaussian surface. From the renormalization-group (RG) arguments<sup>31,32</sup> in a mean-field approximation,<sup>33</sup> the stiffness is derived in the form

$$K_x = \alpha\kappa^3 l \exp\left(-\frac{2\kappa l}{2+\omega}\right) \quad (16)$$

for  $\omega \leq 2$  with the dimensionless parameter

$$\omega \equiv \frac{\hbar\kappa^2}{4\pi\sqrt{m\gamma}}, \quad (17)$$

which represents strength of quantum effects.

On the other hand, if the quantum wall-fluctuation is large, i.e.  $\omega \gg 1$ , the hard-core repulsion becomes important, producing *steric* force between walls.<sup>6</sup> For the mean-field argument<sup>33</sup>, in which one surface is confined in a limited space between perfectly plane two walls with distance  $2l$ , a rigorous proof shows that the effective entropic repulsion decays exponentially.<sup>34</sup> From rescaling  $u' = u/l$  and  $\tau' = c\tau$ , it comes out that the dimensionless parameter of surface configuration is  $\hbar/(l^2\sqrt{m\gamma})$ . We, hence, conclude that  $K_x$  depends on  $l$  for large  $l$  in the form

$$K_x \simeq \exp\{-c_2(m\gamma)^{1/4}l/\sqrt{\hbar}\}, \quad (18)$$

where  $c_2$  is a positive constant. This is consistent with the form derived from RG arguments<sup>32</sup> (see also Appendix A)

$$K_x \simeq \left(\frac{\kappa^2}{\omega}\right)^{11/8} l^{3/4} \exp\left(-\frac{\kappa l}{\sqrt{2\omega}}\right), \quad (19)$$

which is valid for  $\omega \geq 2$ . Note that the above result is derived in a kind of "mean-field" approximation.<sup>33</sup> Recently Zaanen<sup>22</sup> treated fluctuations of many walls in the harmonic approximation and estimated the stiffness between walls from Helfrich's self-consistent condition.<sup>35</sup> In the large- $l$  limit, his result shows the stretched exponential form  $K_x \simeq \exp\{-c_3(\sqrt{m\gamma}/\hbar)^{1/3}l^{2/3}\}$ , where  $c_3$  is a positive constant. It might be unclear whether his argument gives the exact result at the delicate dimensionality ( $d = 2$ ), where the Gaussian surface is in the upper critical dimension  $D (= d+1) = 3$ . In the moderate distance  $l$ , however, the self-consistent condition gives the same exponential form as eq. (19). Since the difference between the simple exponential and stretched exponential forms appears only in an extremely large-spacing region, we use the simple exponential one in the following discussions.

The large  $m$  and small  $m$  regions in which the original exponential repulsion and the hard-core one dominate, respectively, can be defined from the behavior of the deviation  $\Delta u$  of the displacement. Using the mean-field

approximation<sup>33</sup> and applying the harmonic approximation to the potential created by exponential repulsions between adjoining walls, we have the Hamiltonian of a single wall

$$H = \frac{1}{2} \int dy \left\{ \frac{p^2}{m} + \gamma(\partial_y u)^2 + M^2 u^2 \right\} \quad (20)$$

with  $M^2 = 2\alpha\kappa^3 \exp(-\kappa l)$ . The deviation of  $u$  in the harmonic approximation is estimated as

$$[(\Delta u)^2]_{\text{h.a.}} = \frac{\hbar c}{4\pi\gamma} \log\left(\frac{\pi^2\gamma}{a^2 M^2}\right) \approx \frac{\omega l}{\kappa} \quad (21)$$

for large  $l$ . On the other hand, if the quantum string wanders a lot and repels from the adjoining straight lines by the hard-core repulsion, the deviation is proved<sup>34</sup> to be  $(\Delta u)^2 \sim l$ . Since the deviation  $(\Delta u)^2$  has length dimension as  $l^2$ , it should be scaled as  $(\Delta u)^2 = l^2 F(\hbar/l^2 \sqrt{m\gamma})$ . To incorporate the  $l$  dependence for large  $l$ , we set  $F(x) \sim \sqrt{x}$ . The quantum wall with hard-core repulsion, thus, has the deviation

$$[(\Delta u)^2]_{\text{h.c.}} \approx \frac{\sqrt{\omega} l}{\kappa}. \quad (22)$$

By comparison with  $[(\Delta u)^2]_{\text{h.a.}}$  and  $[(\Delta u)^2]_{\text{h.c.}}$ , it is clear that, for  $\omega \ll 1$ , the deviation of the wall in the harmonic potential is small enough and the hard-core repulsion does not work, i.e., the wall is controlled by the exponential repulsion, while for  $\omega \gg 1$  the hard-core repulsion controls the wall wandering and the steric interaction works. This result is consistent with that from RG treatments in the large  $l$  limit,<sup>31,32</sup> where the relevant interaction changes from the exponential one [eq. (16)] to the hard-core one [eq. (19)] at  $\omega = 2$ . This change of dominant interactions is a crossover for moderate  $l$ .

Here we start discussion of the phase diagram. In sec. II B, we showed that stripes become short-range ordered in  $(\tilde{K}_x \tilde{K}_y \tilde{K}_\tau)^{1/3} \hbar^{-1} < C$ , where  $C$  is a constant of order unity. Inserting eqs. (11), (16), and (19) into this criterion, we conclude that the stripes melt for large  $l (> l_c)$  and become a short-range ordered state, i.e., a stripe liquid. (Though this equation is satisfied by two values of  $l_c$ , this equation is asymptotically correct in the large  $l$  limit and hence large  $l_c$  is the physically meaningful one.) We expect that this conclusion does not rely on the approximation method we employed. Even if the steric force decays in a stretched exponential form, this statement still holds. The phase diagram of the stripe solid and liquid phases is shown in Fig. 3 for various mass  $m$ . In the large-mass limit, which corresponds to the classical system, there is no liquid phase. For large  $m$ , the critical length at the melting transition is

$$l_c \simeq \frac{1}{\kappa} \log \frac{Q^7 \sqrt{\gamma} m^{3/2}}{a \hbar^3 \kappa^5} \quad (23)$$

and it rapidly shrinks with reducing the mass  $m$ . Due to a crossover of interactions from the exponential one

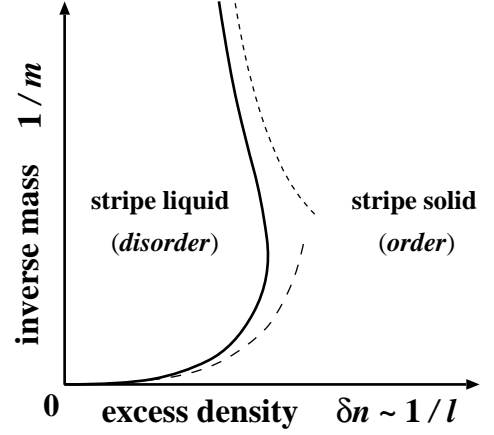


FIG. 3: Possible phase diagram of stripes. The dotted line and dashed one denote asymptotic forms of the phase boundary for small  $m$  [eq. (24)] and large  $m$  [eq. (23)], respectively.

to the steric one, the critical length turns to increase for small  $m$ , satisfying

$$l_c \simeq \frac{\sqrt{\hbar}}{\sqrt{2\pi}(\gamma m)^{1/4}} \log \frac{Q^7 \gamma^{3/4}}{a m^{1/4} \hbar^{3/2} \kappa^{33/16}}. \quad (24)$$

The phase boundary, thus, shows reentrant behavior with changing the parameter  $1/m$ .

From the above calculations, we also obtain the zero-point energy of striped domain walls described by the Hamiltonian (3). Using eqs. (16) and (19), the zero-point energy of stripes per area is estimated as follows<sup>32</sup> (see appendix A): For small  $m$ , i.e.,  $\omega \gg 1$ ,

$$\Delta E_s \simeq \frac{\zeta_0}{l} + \frac{c_4 \sqrt{\gamma}}{a l^{5/4}} \left( \frac{\hbar}{\sqrt{\gamma m}} \right)^{5/8} \exp \left\{ - \left( \frac{2\pi \sqrt{\gamma m}}{\hbar} \right)^{1/2} l \right\}, \quad (25)$$

where  $\zeta_0$  denotes the zero-point energy of one wall per length given by  $\zeta_0 = (\hbar\pi/4a^2)\sqrt{\gamma/m}$  and  $c_4$  is a positive constant, and for large  $m$ , i.e.,  $\omega \ll 1$ ,

$$\Delta E_s \simeq \frac{\zeta_0}{l} + \frac{\hbar c_1 \kappa^2}{8\pi \sqrt{m\gamma}} \exp \left( - \frac{2\kappa l}{2 + \omega} \right). \quad (26)$$

In this approximation, the C-IC transition is of second order and the chemical potential dependence of the excess density is  $\delta n \sim 1/l \sim [-\log(\zeta - \zeta_0)]^{-1}$  for any  $m$ . If the stretched exponential form is adopted as the steric interaction,  $\delta n \sim [-\log(\zeta - \zeta_0)]^{-3/2}$  for small  $m$ . This critical behavior may be modified if dislocations of stripes are taken into account. In an exactly solvable 2D classical domain-wall model, Bhattacharjee<sup>36</sup> showed that dislocations can induce a crossover and change the nature of the C-IC transition. This problem will not be discussed further in this paper.

### D. Comparison with experiments

The present argument on quantum melting of stripes are rather general and hence can be applied to various 2D systems that have incommensurate stripe structures, e.g., adsorbed atoms on graphite and doped high- $T_c$  cuprates. Comparing with experiments done for various adsorbed atoms, we realize that quantum melting of stripes seems to have been already observed in scattering experiments of  $H_2/Gr$  and  $D_2/Gr$ ,<sup>21</sup> where the correlation length shows a sudden decrease in a finite density region just above the commensurate density, though this region has not been regarded as the stripe liquid phase previously.

We can also find a signal for melting of the stripe structure in scattering experiments<sup>15,17</sup> on  $La_{2-x}Sr_xCuO_4$ , where the width of incommensurate peaks becomes larger with lowering the hole density in  $x < 1/8$ . To understand the Sr-concentration dependence of the peak width, we might need to take into account the strength and form of interactions more carefully. The case of power-decay interactions is discussed in Sec. V. It should be noted that effects of randomness are important in some experiments. Bogner and Scheidl<sup>37</sup> discussed that randomness can also make stripes short-range ordered for any wall spacing.

### III. HONEYCOMB PHASE

In this section we discuss quantum fluctuations of the honeycomb structure. First, we consider local lattice vibrations. Since each straight line has finite length  $l$  in hexagons, the zero-point energy of one domain wall has a finite-size correction

$$\Delta\zeta_0(l) = -\frac{\pi\hbar}{16}\sqrt{\frac{\gamma}{m}}\frac{1}{l^2}. \quad (27)$$

There are also so-called “breathing modes”,<sup>4</sup> in which the classical energy except interactions does not change with enlarging one hexagon. In quantum mechanics, this degree of freedom creates a zero-point oscillation and hence increases the energy. If the mass  $m$  is large and the deviation of  $u$  is very small, the potential from the adjoining parallel walls can be well approximated by a quadratic form and in the absence of meandering of walls, breathing of one hexagon behaves as a harmonic oscillator. The zero-point energy per cell is thus roughly estimated in the exponential decay form  $\exp(-\sqrt{3}\kappa l/2)$  for large  $m$ . On the other hand, the hard-core repulsion is dominant for small  $m$ . In the harmonic approximation the problem is reduced to a quantum particle in the square well infinite potential and the energy decays as  $1/(ml^3)$  per cell.

Global lattice vibrations of the honeycomb structure can be treated with a continuum elastic theory, in which the displacement vector  $\mathbf{u} = (u_x, u_y)$  of domain walls (or

intersections) obeys the Hamiltonian

$$H = \frac{1}{2} \int d^2r \left\{ \frac{\sqrt{3}l}{2m} \mathbf{p}^2 + \frac{\mu}{2} (\partial_i u_j + \partial_j u_i)^2 + \lambda (\nabla \cdot \mathbf{u})^2 + \gamma' (\nabla \times \mathbf{u})^2 \right\}. \quad (28)$$

UV cutoffs of the vibrations are set as  $\Delta x = \Delta y = Ql$ . The time cutoff for the longitudinal mode is given by  $\Delta\tau = a/c_l$  with  $c_l^2 = \sqrt{3}l(\mu + \lambda/2)/m$ , and for the transverse mode  $\Delta\tau = a/c_t$  with  $c_t^2 = \sqrt{3}l(\mu + \gamma')/2m$ . The Lamé coefficient  $\gamma'$  can be estimated as  $\gamma' = 2\gamma/\sqrt{3}l$  from the anisotropy of the substrate, where  $\gamma$  is the same interfacial stiffness as in stripes. Other coefficients  $\mu$  and  $\lambda$  are determined from the similar procedure as that for the stripe structure.

In the large- $m$  limit, the Lamé coefficients  $\mu$  and  $\lambda$  are determined by the exponential repulsion in the form

$$2\mu + \lambda \simeq (54\alpha\kappa^3/\pi^2)l^3 \exp(-\sqrt{3}\kappa l). \quad (29)$$

For small  $m$ , the hard-core repulsion between walls (and intersections) creates a steric force. To estimate Lamé coefficients  $\mu$  and  $\lambda$  due to this steric force, we extend Helfrich’s idea<sup>35</sup> to this problem: We made a self-consistent condition

$$l^2 \frac{\partial^2 \Delta e(\mu, \lambda)}{\partial l^2} = 4(\mu + \lambda), \quad (30)$$

where  $\Delta e(\mu, \lambda) = e(\mu, \lambda, \gamma') - e(0, 0, \gamma')$  and  $e(\mu, \lambda, \gamma')$  denotes the energy of eq. (28) given by

$$e(\mu, \lambda, \gamma') = \frac{\hbar\pi^2}{12l^3} \sqrt{\frac{\sqrt{3}\mu l}{2m} + \frac{\gamma}{m}} + \frac{\hbar\pi^2}{12l^3} \sqrt{\frac{\sqrt{3}(2\mu + \lambda)l}{2m}}. \quad (31)$$

Under the assumption  $\mu = b\lambda$ , eq. (30) is solved in the form

$$\mu = b\lambda \approx \left( \frac{35\pi^5}{12} \right)^2 \frac{\sqrt{3}b(b+1/2)}{(b+1)^2} \frac{\hbar^2}{ml^5}, \quad (32)$$

where the ratio  $b$  cannot be determined. This form implies that the wall-wall (or intersection-intersection) interaction effectively decays in the power decay form  $1/l^3$ . From these Lamé coefficients, and using eqs. (27) and (31), the zero-point energy is estimated. For large  $l$ , the leading order term of the energy from the global modes is more dominant than the one that comes from the breathing mode for any  $m$ . The breathing oscillation, thus, gives a soft mode at  $T = 0$ . The most dominant term of the zero-point energy is

$$\Delta E_h \simeq \frac{2\Delta\zeta_0(l)}{\sqrt{3}l} + \frac{\hbar\pi^2}{12l^3} \sqrt{\frac{\gamma}{m}} \quad (33)$$

for any  $m (< \infty)$ , i.e. regardless of forms of the dominant interaction. The second term can be considered as the zero-point energy of torsion vibrations of hexagons.

This system has two components  $(u_x, u_y)$  in  $xy$  plane and hence has similar degrees of freedom as vortex melting problems in 3D superconductors at finite temperature, in which it has been argued that the transition is of first order.<sup>38,39</sup> We, hence, expect that the quantum melting of the honeycomb structure at  $T = 0$  is also of first order and one cannot reach a critical region. Nevertheless it is instructive to derive the phase boundary assuming a second-order transition. In the 2D melting problem, the leading-order term of the bare stiffness<sup>5,40</sup> is given by  $(Ql)^2\mu[(\mu + \lambda)/(2\mu + \lambda) + 1]$  and that becomes  $(Ql)^2\mu$  in the strong anisotropy limit whatever  $b$  is. The most dominant stiffness, thus, comes from  $\mu$  in the 2D plain. In the 2+1D system, after the rescaling  $x' = ax/Ql$ ,  $y' = ay/Ql$ ,  $\mathbf{u}' = 2\pi\mathbf{u}/Ql$ , and  $\tau' = c_t a\tau/Ql$  for the transverse mode and  $\tau' = c_l a\tau/Ql$  for the longitudinal one, the effective action has the bare stiffness

$$\tilde{K}_l = Q^2 l m c_l / \sqrt{3} (2\pi)^2 \quad (34)$$

for the longitudinal mode, and

$$\tilde{K}_t = Q^2 l m c_t / \sqrt{3} (2\pi)^2 \quad (35)$$

for the transverse one. We expect that, even in the 2+1D system, the most dominant contribution to the stiffness in  $xy$  plane comes from  $\mu$  and the effective coupling constant is presumably given by

$$\tilde{K} \approx Q^2 l \sqrt{l m \mu} / 3^{1/4} (2\pi)^2 \sim \hbar Q^2 / l \quad (36)$$

in the strong anisotropy limit ( $\mu, \lambda \ll \gamma'$ ). This indicates that the honeycomb structure is unstable for  $\tilde{K}/\hbar < C$  with a constant  $C$  of order unity, and hence it melts for large  $l$  region.

#### IV. PHASE DIAGRAMS FOR ADSORBED ATOMS

From the above arguments, we obtain phase diagrams for incommensurate phases of adsorbed atoms.<sup>41</sup> A phase diagram with the parameters  $m^{-1}$  and  $\delta n$  was shown in Fig. 1(a) for a positive but not very large intersection energy  $f_I$ . Various phase diagrams can appear depending on the intersection energy  $f_I$ , which is determined by microscopic atomic configurations around intersections.

The stripe liquid phase exists for any mass in the vicinity of the onset of the C-IC transition and no direct transition can occur from the commensurate phase to the stripe ordered one. Actually this stripe liquid phase was presumably observed in  $H_2$  and  $D_2$  on graphite,<sup>21</sup> as already mentioned in Sec. IID. The phase boundary between the stripe liquid and stripe (ordered) solid phases shows a second-order transition in the 3D XY universality class. The phase boundary shows a reentrant behavior because of the crossover of dominant interactions

around  $\omega \approx 2$  as discussed in Sec IIC. The crossover mass can be roughly estimated from  $\omega_c = 2$ . For this purpose, we use the value of the domain-wall width  $\kappa^{-1}$  estimated by Villain<sup>4</sup> as  $\kappa^{-1} = 5a$  for  $^3\text{He}$  monolayer on graphite. The stiffness  $\gamma$  comes from the domain-wall energy and it should be of the same order as the melting temperature of the commensurate phase. We hence set  $a\gamma \approx$  a few [K] and then roughly estimate that the crossover mass ( $am_c \approx a\hbar^2\kappa^4/4(4\pi)^2\gamma$ ) is about  $10^{-4}$  [atomic mass unit] in monolayer on graphite. We note that this value can vary greatly by changing the substrate potential.

If the intersection energy  $f_I$  is not very large, this melting line merges into the phase boundary between the stripe and honeycomb phases. Because the transition from the stripe phase to the honeycomb one is of first order, the system shows a phase separation, in which two phases coexist, for a certain density region (the shaded ones in Fig. 1). From comparison of the zero-point energies of two phases, this phase boundary slightly moves to higher density region with lightening the mass. Moreover, in the small-mass limit, commensurate domains themselves would melt and become a conventional isotropic liquid. This isotropic liquid phase is also taken into account in Fig. 1.

Another quantum correction might appear in the width  $\kappa^{-1}$  of domain walls. Halpin-Healy and Karder<sup>8</sup> argued that, in light atoms, the commensurate solid is more compressible due to quantum fluctuations and the width  $\kappa^{-1}$  becomes small, whereas, in heavy atoms, the width  $\kappa^{-1}$  is large. This is consistent with the estimates from experiments, where the width was estimated as  $\kappa^{-1} \approx 0.8a$  for  $D_2$  systems<sup>21</sup> and  $\approx 5.7a$  for Kr systems.<sup>42</sup> In real adsorbed systems, it is hence likely that due to  $m$ -dependence in  $\kappa^{-1}$  the honeycomb phase is favored for heavy atoms and the stripe phase for light atoms [see Fig. 1(b)].

#### V. STRIPES WITH LONG-RANGE INTERACTIONS

In this section we consider the case that stripes are repelling with each other by long-range interactions with a power-decay form. For example, in doped antiferromagnets, if holes are perfectly doped only in domain walls and domains are insulating, there must be Coulomb long-range repulsion between hole-rich domain walls.

Let us consider the power-decay interaction  $V(u) = c_1 u^{-q+1}$  between walls, where  $c_1$  is a positive constant. (Coulomb repulsion between lines corresponds to  $q = 1$ , i.e.  $V(u) = -\ln u$ .) In the case of Coulomb repulsion, however, the plasma modes  $\omega_p \sim \sqrt{k_x}$  appear and low-lying excitations in  $k_x$ -direction does not have  $k$ -linear spectrum. The plasma modes appear for the long-range interactions  $r^{-q+1}$  with  $q \leq 2$  (see Appendix B). Hence for stripes with  $q \leq 2$ , the stiffness  $K_x$  diverges and the elastic theory with the Hamiltonian (3) cannot be

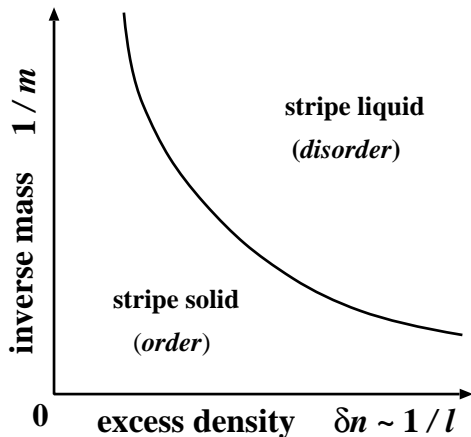


FIG. 4: Phase diagram of the stripe structure with long-range interaction  $r^{-q}$  with  $2 < q < 5$ .

applied. Hereafter, we consider only the case  $q > 2$  and use the melting criterion derived in sec. IIB. The renormalization-group equation<sup>47</sup> shows that power-law repulsions are not modified by the entoropical force from the hard-core repulsion. The stiffness  $K_x$  of the Hamiltonian (3) is hence given by

$$K_x = c_2 l^{-q} \quad (37)$$

with  $c_2 > 0$  for any parameter  $\omega$ . After the rescaling  $\tilde{u} = 2\pi u/Ql$ ,  $\tilde{\tau} = c\tau$ , and  $\tilde{x} = ax/Ql$ , we have the effective coupling

$$\tilde{K}_x = \frac{Qac_2}{4\pi^2 cl^{q-1}} \quad (38)$$

for the effective action (10).

Inserting eq. (38) into eq. (13), we find that the critical point  $l_c$  satisfies

$$\begin{aligned} & (\tilde{K}_x \tilde{K}_y \tilde{K}_\tau)^{1/3} \Big|_{l=l_c} \hbar^{-1} \\ &= \frac{1}{4\pi^2 \hbar} \left\{ \frac{Q^7 l_c^{5-q} \gamma^{1/2} m^{3/2} c_2}{a} \right\}^{1/3} = C, \end{aligned} \quad (39)$$

where  $C$  is a positive constant of order unity. From the melting criterion, we thus find that stripes with  $2 < q < 5$  melt for small-wall-spacing (high-density) region and stabilize for large-wall-spacing (low-density) region because of long-range repulsion. Note that this behavior is contrary to the short-range case. A phase diagram is shown in Fig. 4. This tendency to solidification in low-density region is similar to that of charged point objects, e.g. Wigner crystals, and may be universal in systems with Coulomb repulsion. On the other hand, for  $q > 5$  the tendency to striped ordering is the same as the short-range interaction system and stripes become a liquid for low-density region.

## VI. DISCUSSIONS

To summarize, we studied the effect of quantum fluctuations on 2D domain walls and showed a quantum-melting behavior. We found that striped domain walls with short-range interactions become a stripe liquid even at zero temperature in the incommensurate phase in the vicinity of the onset of C-IC transition. We discussed both short-range and long-range interactions that decay in power laws. It was revealed that striped correlation is enhanced in high density for the case of short-range interactions and in low density for the case of long-range interactions. Though we employed various approximations in estimating the stiffness  $K_x$ , we believe that the above qualitative conclusion does not drastically depend on the choice of approximations.

We discussed mass dependence of domain-wall structures in adsorbed atoms and obtained phase diagrams as shown in Fig. 1. For this purpose, we assumed that the intersection energy is positive. Recently Morishita and Takagi<sup>43</sup> performed path-integral Monte Carlo simulations for  $^3\text{He}$  on graphite. Their result is consistent with the positive intersection energy. They also proposed a honeycomb-cage structure where commensurate regions and discommensurate ones are opposite to the honeycomb incommensurate structure.<sup>44</sup> Direct STM measurements of  $^3\text{He}$  atoms in the incommensurate phase are desired to clarify the real structure.<sup>45</sup> As we commented in Sec. IV, the quantum correction to the domain-wall width  $\kappa^{-1}$  may be also important to reproduce precise phase diagrams of incommensurate adsorbed atoms on graphite. Evaluation of  $m$  dependence of  $\kappa$  remains to be considered.

In a doped Mott insulator, Kivelson *et al.*<sup>20</sup> discussed appearance of electronic nematic and smectic phases from an analogy of classical liquid crystals. From the symmetry, the stripe liquid we discussed is characterized as a nematic state. Our arguments thus demonstrated appearance of a quantum nematic state at  $T = 0$  for low-density region and the correlation length to be finite until zero temperature even in pure systems. A quantum transition from the electronic nematic phase to isotropic Fermi liquid was also discussed by Oganessian *et al.*<sup>46</sup>

Finally, we comment implication of our results on the doping dependence of the incommensurate order observed in  $\text{La}_{2-x}\text{Sr}_x\text{CuO}_4$ .<sup>15,17</sup> Since incommensurability is proportional to Sr concentration  $x$  in the region  $x < 1/8$ , our domain-wall model can be applied in this region. The system is in the insulating spin-glass phase for  $x < 0.055$  and the superconducting phase for  $x > 0.055$ . The correlation length gradually decreases with increasing Sr-concentration  $x$  from  $x \approx 0.024$  and after the system enters into the superconducting phase the correlation length turns to increase. If we assume that antiferromagnetic domains are insulating in the spin-glass phase and metallic in the superconducting one (above  $T_c$ ), the wall-wall interaction would show the power-decay and exponential ones, respectively. Under this assumption, the



hole-density dependence of the correlation length can be naturally understood from the present results. More precisely, in Coulomb repulsive systems the stiffness  $K_x$  is infinite in pure systems due to plasma modes and randomness would be relevant to make the correlation length finite<sup>37</sup>. Another possibility would be that, antiferromagnetic domains are always insulating for  $x < 1/8$  and there is power-decay force between stripes. In that case, to understand enhancement of the correlation length in  $0.055 < x < 1/8$ , we may need to consider that the wall-wall interaction is enhanced in the superconducting phase due to coupling with fluctuations of superconductivity. This is a current hot topic, but out of scope of the present paper.

### Acknowledgments

The author would like to thank Hiroshi Fukuyama, D. R. Nelson, E. Demler, Y. Ohashi, Y. Nishiyama, H. Yoshino, M. Morishita and M. Fujita for stimulating discussions. He also acknowledges kind hospitality of the condensed matter theory group in Harvard University, where this research was partially done. This work was supported in part by Monbusho (MEXT) in Japan through Grand Nos. 13740201 and 1540362.

### APPENDIX A: RENORMALIZATION-GROUP TREATMENT OF A STRING BETWEEN FLAT WALLS

Using the functional renormalization-group treatment given by Fisher and Huse,<sup>47</sup> we reexamine the calculation of effective potential between a quantum string and a flat wall given in Ref. 32. For completeness, we briefly show

the calculation. Instead of using the external potential used in Ref. 32, we consider a valley potential

$$V(x) = \begin{cases} A, & |x| > l, \\ B \exp\{-\kappa(x+l)\} + B \exp\{-\kappa(l-x)\}, & |x| < l, \end{cases} \quad (\text{A1})$$

where the spacing  $l$  between the string and walls is fixed in advance. Rescaling the imaginary time  $\tau$  as  $c\tau$  with  $c = \sqrt{\gamma/m}$ , we have the isotropic effective action for one quantum string in the potential

$$S = \frac{\sqrt{m\gamma}}{2\hbar} \int d\tau dy \{(\partial_\tau u)^2 + (\partial_y u)^2 + \gamma^{-1} V(u)\}. \quad (\text{A2})$$

Integrating out fast modes in string fluctuation up to UV cutoff  $\Delta\tau = \Delta y = \xi$ , we obtain the renormalized action

$$S^R = \frac{\sqrt{m\gamma}}{2\hbar} \int dt dy \{(\partial_\tau u)^2 + (\partial_y u)^2 + \gamma^{-1} V_\xi(u)\} \quad (\text{A3})$$

with the renormalized potential<sup>47</sup>

$$V_\xi(u) = \frac{1}{\sqrt{2\pi}\delta(l^*)} \int_{-\infty}^{\infty} du' V(u') \exp\left\{-\frac{(u-u')^2}{2\delta^2(l^*)}\right\}, \quad (\text{A4})$$

where  $\delta(l^*) = \hbar l^*/\pi\sqrt{m\gamma}$  and  $l^* = \log(\xi/a)$ . The correlation length is determined by<sup>31</sup>

$$\left. \frac{\partial^2 V_\xi(u)}{\partial u^2} \right|_{u=0} = \frac{\gamma}{\xi^2}. \quad (\text{A5})$$

One can evaluate the renormalized potential using the steepest-descent method in the large- $l$  limit. For  $\omega (= \hbar\kappa^2/4\pi\sqrt{m\gamma}) > 2$ ,

$$\begin{aligned} V_\xi(u) = & \sqrt{\frac{l^*\omega}{\pi}} \left\{ \frac{A}{\kappa(l+u)} + \frac{B}{2l^*\omega - \kappa(l+u)} \right\} \exp\left\{-\frac{\kappa^2}{4l^*\omega}(l+u)^2\right\} \\ & + \sqrt{\frac{l^*\omega}{\pi}} \left\{ \frac{A}{\kappa(l-u)} + \frac{B}{2l^*\omega - \kappa(l-u)} \right\} \exp\left\{-\frac{\kappa^2}{4l^*\omega}(l-u)^2\right\}. \end{aligned} \quad (\text{A6})$$

The condition (A5) gives the correlation length in the leading order

$$\xi = \sqrt{a} \left( \frac{\gamma^2 \omega^{3/2} l}{\kappa^3} \right)^{1/8} \exp\left( \frac{\kappa l}{2\sqrt{2\omega}} \right) \quad (\text{A7})$$

and the renormalized potential  $V_\xi$  at the equilibrium po-

sition  $u = 0$

$$V_\xi(u) \Big|_{u=0} = \frac{A}{a\sqrt{\pi}} \left( \frac{2\kappa^3 \gamma^2}{\omega^{3/2} l} \right)^{1/4} \exp\left( -\frac{\kappa l}{\sqrt{2\omega}} \right), \quad (\text{A8})$$

where the exponents of the power forms in eqs. (A7) and (A8) are different from those in Ref. 32.

For  $\omega < 2$ ,  $V_\xi(u)$  is calculated as

$$\begin{aligned} V_\xi(u) &= \frac{\sqrt{l^*\omega}A}{\sqrt{\pi\kappa}(l+u)} \exp\left\{-\frac{\kappa^2}{4l^*\omega}(l+u)^2\right\} \\ &+ \frac{\sqrt{l^*\omega}A}{\sqrt{\pi\kappa}(l-u)} \exp\left\{-\frac{\kappa^2}{4l^*\omega}(l-u)^2\right\} \\ &+ B \exp\{-\kappa(l+u) + l^*\omega\} \\ &+ B \exp\{-\kappa(l-u) + l^*\omega\}. \end{aligned} \quad (\text{A9})$$

The condition (A5) leads to the correlation length

$$\xi = a \left( \frac{\gamma}{2B\kappa^2 a^2} \right)^{1/(2+\omega)} \exp\left( \frac{\kappa l}{2+\omega} \right) \quad (\text{A10})$$

and the renormalized potential at the equilibrium position  $u = 0$

$$V_\xi(u) \Big|_{u=0} = 2B \left( \frac{\gamma}{2B\kappa^2 a^2} \right)^{\omega/(2+\omega)} \exp\left( -\frac{2\kappa l}{2+\omega} \right). \quad (\text{A11})$$

These are the same as the previous ones.<sup>32</sup>

## APPENDIX B: ELASTIC THEORY OF STRIPES WITH LONG-RANGE INTERACTIONS

If we have a stripe structure of walls displaced slightly from equilibrium, then the additional potential energy is

$$\Delta E = \frac{1}{2} \sum_{\mathbf{r}_i \neq \mathbf{r}_j} |\mathbf{r}_i - \mathbf{r}_j|^{-q}, \quad (\text{B1})$$

where

$$\sum_{\mathbf{r}_i} \equiv \sum_i \int dy_i \quad (\text{B2})$$

and

$$\mathbf{r}_i = (il + u_i(y_i), y_i). \quad (\text{B3})$$

Here  $u_i(y_i)$  denotes displacement at  $y = y_i$  in  $i$ th wall. If the displacements are small, we can expand the energy in powers of  $u$  and obtain<sup>48,49</sup>

$$\Delta E = \frac{1}{2} \sum_{\mathbf{r}_i, \mathbf{r}_j} \Pi(\mathbf{r}_i, \mathbf{r}_j) u(\mathbf{r}_i) u(\mathbf{r}_j), \quad (\text{B4})$$

where  $u(\mathbf{r}_i) = u_i(y_i)$ . We can Fourier transform (B4) to obtain

$$\Delta E = \frac{1}{2(la)^2} \int \frac{d^2 p}{(2\pi)^2} \Pi(\mathbf{p}) |u(\mathbf{p})|^2 \quad (\text{B5})$$

and

$$\begin{aligned} \Pi(\mathbf{p}) &= la \lim_{z \rightarrow 0} \frac{\partial^2}{\partial z^2} \sum_{\mathbf{r}} \frac{1 - \exp(-ip_x r_x)}{|z\mathbf{e}_x - \mathbf{r}|^q} \\ &= \begin{cases} \frac{2\pi^{3/2}\Gamma((q-1)/2)}{(q-2)\Gamma(q/2)^2 l^{q-2}} p_x^2, & q > 2, \\ c_1 p_x^2 \log p_x, & q = 2 \\ c_2 |p_x|, & q = 1 \end{cases} \end{aligned} \quad (\text{B6})$$

for small  $p_x$ , where  $c_1$  and  $c_2$  are positive constants. On the other hand, in the elastic theory, potential energy is written as

$$\Delta E = \frac{K_x}{2} \int \frac{d^2 p}{(2\pi)^2} |p_x|^2 |u(\mathbf{p})|^2. \quad (\text{B8})$$

Thus if the exponent satisfies  $q > 2$ , we can describe excitations with the elastic theory of Gaussian forms and, if  $q \leq 2$ , we cannot because  $K_x$  diverges.

- 
- <sup>1</sup> For a review, see P. Bak, Rep. Prog. Phys., **45**, 587 (1982).  
<sup>2</sup> V. L. Pokrovsky and A. L. Talapov, Phys. Rev. Lett. **42**, 65 (1979).  
<sup>3</sup> P. Bak, D. Mukamel, J. Villain and K. Wentowska, Phys. Rev. B **19**, 1610 (1979).  
<sup>4</sup> J. Villain, in *Ordering in Strongly Fluctuating Condensed Matter Systems*, edited by T. Riste (Plenum, New York, 1980), p221.  
<sup>5</sup> S. N. Coppersmith, D. S. Fisher, B. I. Halperin, P. A. Lee and W. F. Brinkman, Phys. Rev. Lett. **46**, 549 (1982); Phys. Rev. B **25**, 349 (1982).  
<sup>6</sup> M. E. Fisher and D. S. Fisher, Phys. Rev. B **25**, 3192 (1982).  
<sup>7</sup> M. Kardar and A. N. Berker, Phys. Rev. Lett. **48**, 1552 (1982).  
<sup>8</sup> T. Halpin-Healy and M. Kardar, Phys. Rev. B **34**, 318 (1986).  
<sup>9</sup> K. L. D'Amico, D. E. Moncton, E. D. Specht, R. J. Birge-

- neau, S. E. Nagler, and P. M. Horn, Phys. Rev. Lett. **53**, 2250 (1984), and references therein.  
<sup>10</sup> H. Hong, C. J. Peters, A. Mak, R. J. Birgeneau, P. M. Horn, and H. Suematsu, Phys. Rev. B **40**, 4797 (1989).  
<sup>11</sup> H. Wiechert, Physics B **169**, 144 (1991).  
<sup>12</sup> D. S. Greywall, Phys. Rev. B **47**, 309 (1993).  
<sup>13</sup> B. Grimm, H. Hövel, M. Bödecker, K. Fieger, and B. Reihl, Surf. Sci. **454**, 618 (2000).  
<sup>14</sup> J. M. Tranquada, B. J. Sternlieb, J. D. Axe, Y. Nakamura, S. Uchida, Nature (London) **375**, 561 (1995).  
<sup>15</sup> K. Yamada, C. H. Lee, K. Kurahashi, J. Wada, S. Wakimoto, S. Ueki, H. Kimura, Y. Endoh, S. Hosoya, G. Shirane, R. J. Birgeneau, M. Greven, M. A. Kastner, and Y. J. Kim, Phys. Rev. B **57**, 6165 (1998).  
<sup>16</sup> T. Momoi and K. Totsuka, Phys. Rev. B **62**, 15067 (2000).  
<sup>17</sup> M. Fujita, K. Yamada, H. Hiraka, P. M. Gehring, S. H. Lee, S. Wakimoto, and G. Shirane, Phys. Rev. B **65**, 64505 (2002).

- <sup>18</sup> C. Nayak and F. Wilczek, Phys. Rev. Lett. **78**, 2465 (1997).
- <sup>19</sup> H. Eskes, O. Y. Osman, R. Grimberg, W. van Saarloos, and J. Zaanen, Phys. Rev. B **58**, 6963 (1998).
- <sup>20</sup> S. A. Kivelson, E. Fradkin, V. J. Emery, Nature (London) **393**, 550 (1998).
- <sup>21</sup> H. Freimuth, H. Wiechert, and H. J. Lauter, Surf. Sci. **189/190**, 548 (1987); H. Freimuth, H. Wiechert, H. P. Schildberg and H. J. Lauter, Phys. Rev. B **42**, 587 (1990).
- <sup>22</sup> J. Zaanen, Phys. Rev. Lett. **84**, 753 (2000).
- <sup>23</sup> D. R. Nelson and J. Toner, Phys. Rev. B **24**, 363 (1981).
- <sup>24</sup> P. M. Chaikin and T. C. Lubensky, *Principles of condensed matter physics*, (Cambridge Univ. Press, Cambridge, 1997).
- <sup>25</sup> D. R. Nelson, *Phase transitions and critical phenomena Vol. 7* edited by C. Domb and M. S. Green (Academic Press, London, 1976), P. 1.
- <sup>26</sup> J. M. Kosterlitz and D. J. Thouless, J. Phys. C **6**, 1181 (1973).
- <sup>27</sup> R. P. Feynman, *Progress in Low Temperature Physics*, edited by C. J. Gorter (North-Holland, Amsterdam, 1955), Vol. 1.
- <sup>28</sup> G. Kohring, R. E. Shrock, and P. Wills, Phys. Rev. Lett. **57**, 1358 (1986).
- <sup>29</sup> S. R. Shenoy, Phys. Rev. B **40**, 5056 (1989).
- <sup>30</sup> J. C. Le Guillou and J. Zinn-Justin, Phys. Rev. B **21**, 3976 (1980).
- <sup>31</sup> E. Brézin, B. I. Halperin, and S. Leibler, Phys. Rev. Lett. **50**, 1387 (1983).
- <sup>32</sup> D. Sornette, Europhys. Lett. **2**, 715 (1986).
- <sup>33</sup> Here, “mean-field approximation” means that two adjoining walls are set to straight and only fluctuations of a single wall between them are treated.
- <sup>34</sup> J. Bricmont, A. El Mellouki, and J. Fröhlich, J. Stat. Phys. **42**, 743 (1986).
- <sup>35</sup> W. Helfrich, Z. Naturforsch. A **33**, 305 (1978).
- <sup>36</sup> S. M. Bhattacharjee, Phys. Rev. Lett. **53**, 1161 (1984).
- <sup>37</sup> S. Bogner and S. Scheidl, Phys. Rev. B **64**, 054517 (2001).
- <sup>38</sup> E. Brezin, D. R. Nelson, and A. Thiaville, Phys. Rev. B **31**, 7124 (1985).
- <sup>39</sup> G. Blatter, M. M. Feigel'man, V. B. Geshkenbein, A. I. Larkin, and V. M. Vinokur, Rev. Mod. Phys. **66**, 1125 (1994).
- <sup>40</sup> D. R. Nelson and B. I. Halperin, Phys. Rev. B **19**, 2457 (1979).
- <sup>41</sup> Preliminary results of the present arguments were published in T. Momoi, J. Low Temp. Phys. (2002), in press.
- <sup>42</sup> P. W. Stephens, P. A. Heiney, R. J. Birgeneau, P. M. Horn, D. E. Moncton and G. S. Brown, Phys. Rev. B **29**, 3512 (1984).
- <sup>43</sup> M. Morishita and T. Takagi, private communication.
- <sup>44</sup> M. Morishita and T. Takagi, Phys. Rev. Lett. **87**, 185301 (2001).
- <sup>45</sup> T. Matsui, H. Kambara and H. Fukuyama, private communication.
- <sup>46</sup> V. Oganesyan, S. A. Kivelson, and E. Fradkin, Phys. Rev. B **64**, 195109 (2001).
- <sup>47</sup> D. S. Fisher and D. A. Huse, Phys. Rev. B **32**, 247 (1985).
- <sup>48</sup> L. Bonsall and A. A. Maradudin, Phys. Rev. B **15**, 1959 (1977).
- <sup>49</sup> D. S. Fisher, B. I. Halperin, and R. Morf, Phys. Rev. B **20**, 4692 (1979).